Molecular BioSystems

Accepted Manuscript

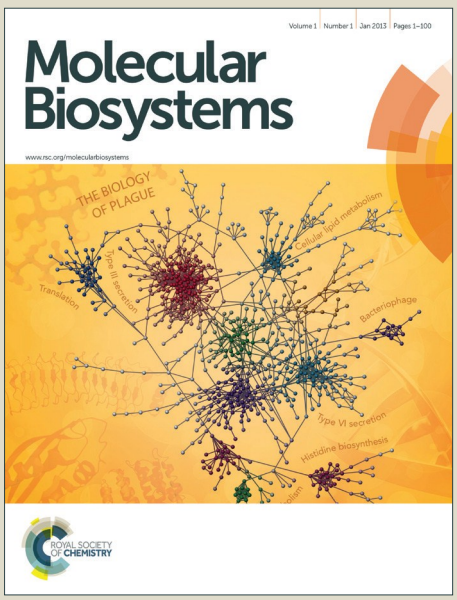

ROYAL SOCIETY OF CHEMISTRY

www.rsc.org/molecularbiosystems

Novelty of the work

In this work we performed the first transcriptional study of a filamentous fungus (*N. crassa*) in response to chitosan.

Graphic

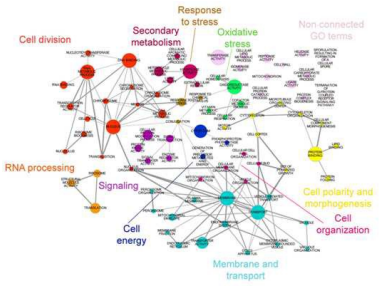

Neurospora crassa transcriptomics reveals oxidative stress and plasma membrane homeostasis biology genes as key targets in response to chitosan

Federico Lopez-Moya[1], David Kowbel[2], Mª José Nueda[3], Javier Palma-Guerrero[2, 4], N. Louise Glass[2] and Luis Vicente Lopez-Llorca[1].

[1]Laboratory of Plant Pathology, Multidisciplinary Institute for Environmental Studies (MIES) Ramon Margalef, Department of Marine Sciences and Applied Biology, University of Alicante, E-03080 Alicante, Spain.

[2]Department of Plant and Microbial Biology, University of California, Berkeley CA, 94720-3120 USA.

[3]Statistics and Operation Research Department, University of Alicante, E-03080 Alicante, Spain.

[4]Current address: Department of Environmental Systems Science, ETH Zurich, Zurich, Switzerland.

Authorship emails:

federico.lopez@ua.es

djkowbel@berkeley.edu

mj.nueda@ua.es

javier.palma@usys.ethz.ch

lglass@berkeley.edu

lv.lopez@ua.es

Correspondig author: federico.lopez@ua.es

Abstract

Chitosan is a natural polymer with antimicrobial activity. Chitosan causes plasma membrane permeabilization and induction of intracellular reactive oxygen species (ROS) in *Neurospora crassa*. We have determined the transcriptional profile of *N. crassa* to chitosan and identified the main gene targets involved in the cellular response to this compound. Global network analyses showed membrane, transport and oxidoreductase activity as key nodes affected by chitosan. Activation of oxidative metabolism indicates the importance of ROS and cell energy together with plasma membrane homeostasis in *N. crassa* response to chitosan. Deletion strain analysis of chitosan susceptibility pointed, NCU03639 encoding a class 3 lipase, involved in plasma membrane repair by lipid replacement and NCU04537 a MFS monosaccharide transporter related with assimilation of simple sugars, as main gene targets of chitosan. NCU10521, a glutathione S-transferase-4 involved in the generation of reducing power for scavenging intracellular ROS is also a determinant chitosan gene target. Ca^{2+} increased tolerance to chitosan in *N. crassa.* Growth of NCU10610 (*fig 1* domain) and SYT1 (a synaptotagmin) deletion strains was significantly increased by Ca^{2+} in presence of chitosan. Both genes play a determinant role in *N. crassa* membrane homeostasis. Our results are of paramount importance for developing chitosan as antifungal.

Keywords

Drug targets, time-series analysis, ROS, membrane remodeling, calcium

Introduction

Chitosan is a polymer obtained by partial chitin N-deacetylation[1] which has antifungal activity.[2] Chitosan inhibits growth of filamentous fungi and yeast human pathogens.[3,4] To develop chitosan as an antifungal treatment, a full understanding of its mode of action is necessary. In *Saccharomyces cerevisiae,* the response to chitooligosaccharides is mediated by proteins associated with plasma membrane, respiration, ATP production and mitochondrial organization.[5] Five genes (*arl1*, *bck2*, *erg24*, *msg5* and *rba50*) were characterized that provided chitosan resistance when overexpressed or increased sensitivity as a deletion strains. These genes have important roles in signaling pathways, cell membrane integrity and transcription regulation.[5] Other transcriptional studies in *S. cerevisiae* revealed the relevance of oxidative respiration, mitochondrial biogenesis and transport in the response to chitosan.[6] Previous physiological studies in *N. crassa* demonstrated that chitosan causes plasma membrane permeabilization.[7] Membrane fluidity is a key factor determining chitosan sensitivity in fungi.[8] Cell energy and mitochondrial activity have also an important role in moderating the antifungal activity of chitosan.[7] The transcriptional response of filamentous fungi to this antifungal remains unknown.

Membrane damage caused by currently used antifungals (eg. azoles) is associated with the induction of intracellular reactive oxygen species (ROS).[9,10] We have recently shown that low chitosan concentration increased intracellular ROS levels in *N. crassa* leading to partial membrane permeabilization.[4] Increasing chitosan dose dramatically raised ROS levels causing full membrane permeabilization and subsequent cell death. Oxidative stress by chitosan is mediated by the energetic status of the cell. A reduction in cell energy by blocking the electron transport chain protected *N. crassa* from chitosan damage.[7] The plasma membrane of *N. crassa* contains high levels of polyunsaturated free fatty acids (FFA), this fact is directly associated with its susceptibility to chitosan.[8] Fungal plasma membrane lipids could be easily oxidized by an induction of intracellular oxidative stress generated by chitosan as found for other antifungals.[10,11] This fact would link ROS and membrane homeostasis biology in the mode of action of chitosan.

Ca^{2+} is known to be involved in plasma membrane repair.[12] Previous molecular studies revealed SYT1, a synaptotagmin, involved in membrane repair in several organisms[13] including *N. crassa*.[14] Moreover, Ca^{2+} plays a role in the response to oxidative stress and programmed cell death in *N. crassa*.[15] PRM1 and FIG1 are key proteins in calcium-dependent plasma membrane remodeling during membrane fusion in *S. cerevisiae* and *N. crassa*.[16-19] In *N. crassa,* two additional proteins, LFD1 and LFD2 are also involved in Ca^{2+}-dependent plasma membrane repair during cell fusion.[14,20] It is currently unknown, however, how fungi repair membrane damage caused by chitosan.

In this work, we analyzed the transcriptional response of *N. crassa* germinating conidia and determined the main gene functions related with the exposure to chitosan. We applied temporal series analysis (Next-maSigPro[21] and ASCA-genes[22]) and a network analysis approach (Cytoscape)[23] to understand the dynamics of functions and gene targets involved in *N. crassa* response to chitosan. This study has pointed mitochondrion (ROS) and membrane homeostasis as the main functions in the response of *N. crassa* to chitosan and has identified key gene targets. Deletion strains of these key genes were evaluated for fitness and growth. We further demonstrated that extracellular calcium protects fungal cells from damage caused by chitosan. These studies are a key step for improving the knowledge on the mode of action of chitosan, which is essential for its future development as antifungal.

Results and Discussion

Chitosan causes an early activation and late repression of *N. crassa* genes

The experimental conditions for analyzing the effect of chitosan on *N. crassa* germination and development are shown in Fig. 1. Time-course of *N. crassa* conidia germination is included in Figure 1A. Germination defects were quantified after 8h exposure of *N. crassa* conidia to 0.5 μg ml^{-1} chitosan (Fig. 1B; IC_{50}) which showed an approximately 50% reduction in germination. This chitosan concentration was used for high throughput transcriptomic study.

To identify transcriptional changes caused by exposure of *N. crassa* to chitosan a 3-stage time-course (4, 8 and 16h post-inoculation) was performed. A total of 523 *N. crassa* genes were considered differentially expressed (p-value < 0.05), with a fold change ≥ 2 (lower fold change values were considered non-significant), in response to chitosan (Fig. 2A). Of these, 55.6% (291 genes) were down-regulated and 45.3% (237 genes) up-regulated. Our time-course experiment showed a progressive reduction in the number of genes whose expression increased upon exposure to chitosan (142 induced genes at 4h, 119 at 8h and 45 at 16h; Fig. 2B). In contrast, exposure to chitosan resulted in an increase in the number of genes whose expression levels decreased over time (79, 93 and 207 genes down-regulated at 4, 8 and 16h, respectively; Fig. 2C). A subset of 22 genes was differentially expressed consistently (p-value < 0.05; $\log_2$foldchange ≥ 2) throughout the whole time-course (Fig. 2A). Most of these genes (19) were down-regulated, two genes were up-regulated and only one gene of this set (NCU05018) had an early (4 and 8h) induction and a late (16h) gene repression (Fig. 2D).

Expression of 10 *N. crassa* genes representative of functional categories that were differentially expressed by exposure to chitosan were selected to validate our RNA-seq analysis. Gene expression was evaluated by qRT-PCR following an 8h exposure to chitosan (Fig S1). These genes were NCU05134, NCU06123, NCU07610, NCU01382 and NCU05712 (involved in response to oxidative stress), NCU02363 (involved in response to chemical compounds), NCU05018, NCU3494 *pin-c* (related with heterokaryon incompatibility and membrane biology), NCU05764 (a sam-dependent methyltransferase) and a transcription factor with a zinc-finger domain (NCU05767). All genes analyzed by qRT-PCR showed an expression pattern consistent with that derived from RNA-seq data analysis (Fig. S1).

N. crassa main gene functions differentially expressed with chitosan are oxidoreductase activity, membrane homeostasis and microtubule organization.

A gene ontology (GO) functional annotation of *N. crassa* genes differentially expressed in response to chitosan was carried out using Blast2GO (Fig. 3 and Figs. S2 and S3). All GO-domains (molecular function, MF; biological process, BP; cell component, CC) and times were considered together for a complete functional gene expression analysis (Fig.

3A). Oxidoreductase activity (70 genes), membrane (57 genes) and transport (44 genes) were the most enriched GO-terms.

Using maSigFun software for RNA-seq data time series analysis combined with GO annotation, we generated the time-course of functional gene expression for the most significantly enriched GO-terms representing *N. crassa* response to chitosan (Fig. 3B). The analysis identified 12 significant GO-terms using FDR=0.05 and R^2=0.4 levels, as suggested in previous studies[24]. Chitosan modified patterns of expression of ROS-related GO terms mitochondrion and peroxisome organization (Fig. 3B). Mitochondrion genes increased expression through time reaching maximum values of expression at 16h, suggesting that chitosan enhances synthesis/turnover of mitochondrion components (respiration). Genes associated with peroxisome organization, involved in ROS degradation and catabolism of free fatty acids, were first highly expressed (4h) then completely repressed (16h). Likewise, chitosan modified patterns of expression of GO categories related with membrane structure and biology. Exposure to chitosan was associated with repression at 16h of genes involved in cell cortex, vesicle organization and conjugation (Fig. 3B). Moreover, G-protein coupled receptor signaling were compromised by chitosan during all the time-course study (Fig. 3B). These features indicate that chitosan significantly compromised both structure and signaling associated with cell membrane homeostasis. Genes associated with GO-terms related to cell growth such as microtubule organizing center and motor activity had decreased expression values by chitosan through time (Fig. 3B). This behavior suggests the importance of cytoskeleton in the antifungal action of chitosan. Conversely, chitosan increased expression of genes associated with GO terms involved in protein synthesis (ribosome and ribosome biogenesis, Fig. 3B). This would support the increasing expression of genes and synthesis of proteins related to oxidoreductase activity by chitosan (Fig. 3A). In a similar way, nucleolus and structural molecule activity (Fig. 3B) genes were also late activated by chitosan.

Potential gene targets of *N. crassa* to chitosan and their dynamics of expression

Initial time-course analysis showed 5% of *N. crassa* genes significantly expressed in response of *N. crassa* to chitosan. A subset of 33 genes with a relevant change (*p*-value

170 < 0.05; $\log_2$fold-change > ±4.5) of expression is shown in Table S1. A restrictive cut-off
171 was applied with the aim of detect the genes with large change in expression in response
172 to chitosan. This subset included the 22 genes found in the differential gene expression
173 analysis (Fig. 2) plus genes highly expressed (at early or late steps) associated with
174 enriched GO-terms after chitosan exposure.

175 When applying ASCA-genes method we focused on submodel (b+ab) that represents
176 67.18% of total variation. Two components were selected, explaining 93% of this
177 variability (52.38% and 40.62%, respectively; Fig. S4). They, therefore, represented the
178 main gene expression in response to chitosan. First component identified a gene
179 expression difference between chitosan and control constant through time (Fig. S4A).
180 Second component identified expression pattern characterized by a clear interaction
181 through time (Fig. S4B). The analysis of the squared prediction error (SPE) and
182 leverage, determined a cut-off using gamma method, revealed 410 genes which
183 followed the selected components (which explained 93% of variation) and 474 with a
184 behaviour not identified in these (Fig. S5). Comparisons between ASCA and the fold-
185 change gene selection methods (523 genes in total) revealed 447 genes in common (Fig.
186 S4C). Summarizes graphically this comparison where is observed a high overlap
187 between fold-change gene selection and genes with high leverage (also scores can be
188 observed). Moreover 33 genes with a relevant change (listed in Table S1) were also
189 identified showing high scores for the two components identified after PCA (Fig.S4C).

190 To inspect ASCA gene selection time series two cluster analyses were applied: one
191 to the well-modelled genes (M) and another to the bad-modelled genes (NM) obtaining
192 4 and 6 clusters respectively (Fig4 and S6). Both analyses were performed with the
193 hierarchical method. Cluster 1M (Fig. 4A) contained genes associated with an early
194 response to chitosan including two dioxygenases: NCU01849, the most highly
195 expressed gene in response to chitosan (11.16 fold-induction) and NCU01071 a
196 predicted 2OG-Fe dioxygenase, both involved in response to oxidative stress.

197 We also found a set of genes mainly associated with plasma membrane, signaling
198 and response to chemical compound (NCU02363; RTA1-like protein). In addition, a
199 plasma membrane protein (*het* domain) associated with intracellular oxidative stress

(NCU07840), hypothetical protein with a C-terminal homeodomain (NCU00733) and hypothetical protein with a peroxisome membrane anchored protein conserved region (NCU04555) which strongly decreased in expression levels in *N. crassa* conidia treated with chitosan. Cluster 4M showed a steady increase of gene expression (Fig. 4D). Genes in this cluster were involved in cell response to oxidative stress (NCU05134 and NCU08907) and a monosaccharide transporter perhaps involved in chitosan assimilation or detoxification (NCU04537, fold-induction 9.27 after 16h growing with chitosan). Besides, other genes related with sugars assimilation were also induces in presence of chitosan such as NCU01633 (*hxt13*; Table S2). Clusters 2M and 3M, had gene expression changes in the control but not in the chitosan treatment (Figs. 4B and 4C). Genes in these clusters were mainly related with fungal reproduction and development and response to oxidative stress. Cluster 2M included two genes associated with membrane homeostasis: NCU03494 (*pin-c*) essential for non-self-recognition and NCU10610, a protein with a *fig 1* domain (Ca^{2+} regulator and membrane fusion) related with cell fusion.

Genes which did not fit the model (NM), with high SPE and leverage in the ASCA analysis, were grouped in 6 clusters including 474 genes (Fig. S6). Cluster 5NM which showed a late activation in presence of chitosan, included genes such as NCU10521 (fold-induction 8.16 at 16h) a glutathione S-transferase-4 possibly involved in the generation of reducing power for scavenging intracellular ROS. Other genes involved in ROS assimilation were also induced at 16h such as NCU05780 (*gst-1*; Table S2). Cluster 3NM included expression of genes such as NCU08770 a hypothetical protein with a histone chaperone domain with slight changes of expression in presence of chitosan (Fig. S6). Cluster 4NM included genes with an early induction (4-8h) and then a reduction of gene expression such as NCU03639, a lipase class 3 involved in lipid, fatty acids and isoprenoid metabolism. The overexpression of this gene suggests its role in plasma membrane homeostasis during chitosan damage.

Other significantly expressed (more than 6 fold-change expression, Table S2) genes in response to chitosan related with the main functions described previously included NCU03213 encoding a predicted mannosyl-phosphorylation protein related with phosphocholine metabolism (lipid modification). Early induction of other genes related

with predicted roles in lipid metabolism such as NCU16960 (geranyl reductase) putative involved in the biosynthesis of plasma membrane lipids were also detected.

N. crassa deletion strains involved in membrane homeostasis and ROS detoxification showed increased sensitivity to chitosan

Fifteen deletion strains of genes highly expressed and associated with enriched GO-terms in response to chitosan were evaluated to identify gene targets in *N. crassa*. Five deletion strains showed increased sensitivity to chitosan (Fig. 5 and Fig. S7). ΔNCU03639 (lipase) and ΔNCU04537 (monosaccharide transporter) were the most sensitive. These deletion strains exhibited a minimal inhibitory concentration (MIC, 3 μg ml^{-1}) lower than the WT (MIC 6 μg ml^{-1}; Fig. 5A). They also showed a 6-8h delay in the start of the exponential growth phase at 2 μg ml^{-1} of chitosan in comparison to the WT (Figs. 5B-5D). Furthermore, ΔNCU10521 (glutathione S-transferase), ΔNCU08907 Clock controller gene 13 (*ccg-13*) and ΔNCU07840 (plasma membrane protein with a *het* domain) were moderately (MIC at 4 μg ml^{-1}) sensitive to chitosan (Fig. 5A). These strains showed a 6-12h delay in the start of exponential growth phase with respect to WT at 3 μg ml^{-1} of chitosan (Fig. S7). ΔNCU10610 (Ca^{2+} regulator with *fig 1* domain) showed the same MIC as WT (6 μg ml^{-1}), but had a delay (8h) in the start of exponential growth phase at 4 μg ml^{-1} chitosan (Fig. S7 and Table S3). Conversely, ΔNCU02363 (RTA1 like-protein) and ΔNCU05134 (hypothetical protein) with the same MIC as the WT, started their exponential phases 7 and 16h earlier than WT (Fig. S7 and Table S3) indicating moderate tolerance of chitosan respect to WT. ΔNCU08770 (hypothetical protein with a histone chaperone domain CHZ) had increased resistance to chitosan (MIC > 6 μg ml^{-1}; Fig. 5E). The start of the exponential growth phase in this deletion strain was 15h earlier than WT at 4 μg ml^{-1} of chitosan (Table S3).

Thirteen deletion strains (mating type a) were crossed to WT (mating type A) to assess meiotic segregation of chitosan sensitivity phenotype with the hygromycin marker. Seggregants of each mutant showed similar chitosan sensitivity than the original deletion strain. In four chitosan gene targets (ΔNCU03639, ΔNCU04537, ΔNCU07840 and ΔNCU10521), segreggants showed the same chitosan antifungal phenotype (MIC) and hygromycin resistance than the original deletion strains.

Ca^{2+} protects *N. crassa* conidia from chitosan damage

Ca^{2+} increased tolerance to chitosan in *N. crassa* (Fig. 6). The WT strain at 0.68 mM $CaCl_2$ with 0.5 μg ml^{-1} chitosan resumed growth 4h earlier than without Ca^{2+} (Figs. 6A). A higher level of $CaCl_2$ (2.72 mM) in the presence of 0.5 μg ml^{-1} chitosan further improved fungal growth with a 7h advance in the start of the exponential phase with respect to *N. crassa* with chitosan and no calcium (Fig. 6A). Increasing $CaCl_2$ concentrations with no chitosan did not affect fungal growth (data not shown).

Conidia in calcium-free medium treated with chitosan (0.5 μg ml^{-1}) were stained (Fig. 6B) with the vital dye propidium iodide (PI) indicating cell mortality. On the contrary, conidia treated with both chitosan (0.5 μg ml^{-1}) and calcium chloride (0.68 mM), this showed no staining remaining alive (Fig. 6C). Similar results were found when increasing chitosan concentrations (Fig. S8). In particular, 0.5, 2.5 and 5 μg ml^{-1} chitosan and $CaCl_2$ treated cells had significantly (p-value < 0.05) lower mortality than conidia treated with chitosan but no calcium.

Treatment with Ca^{2+} also reduced chitosan damage in deletion strain in the locus ΔNCU10610 with a *fig 1* domain and ΔNCU03263 (*syt-1*), both associated with plasma membrane remodeling (Figs. 6D and 6E). Increasing $CaCl_2$ concentration (10 mM to 20 mM) significantly improved growth of WT, ΔNCU10610 and ΔNCU03263 strains in a medium amended with a high amount of chitosan (4 μg ml^{-1}; Figs. 6D and 6E). With less concentration of Ca^{2+} in the medium (0.68 mM), chitosan completely inhibited fungal growth. ΔNCU10610 showed more tolerance to chitosan respect to WT, this strain started exponential phase at 27h, whereas WT strain did so 3h later under the same conditions. ΔNCU03263 was most sensitive to chitosan with high amount of calcium, starting the exponential phase after 35h, with slower growth than WT and ΔNCU10610. When [$CaCl_2$] was increased (20 mM) all strains tested showed higher resistance to chitosan (Fig. 6E). This was especially relevant for ΔNCU03263 which showed a ca. 2 fold growth increase under these conditions (Fig. 6E).

We found in this work that chitosan significantly induced changes of expression of 5% of *N. crassa* genes in the genome. A global Cytoscape network showed membrane and transport as key nodes grouping genes affected by chitosan (Fig. 7). Plasma membrane was connected with cell vesicles and cell wall suggesting the importance of these outer structures and their dynamics in presence of chitosan. Oxidoreductase enhanced node indicated the importance of ROS and cell energy in *N. crassa* response to chitosan.[4,7] Several nodes related with cytoskeleton dynamics indicate that chitosan also affects cell growth (Fig. 7). Other transcriptional studies, using *S. cerevisiae* mutant collections determined genes associated with plasma membrane, respiration, ATP production and mitochondrial organization as main targets of chitooligosaccharides.[5,6]

In this study, we demonstrated that exposure to chitosan increased the expression of genes involved in plasma membrane dynamics such as lipases. Imidazoles and triazoles (e.g. fluconazole, voriconazol and others) mode of action is based on the ergosterol biosynthesis inhibition,[25,26] thereby altering plasma membrane fluidity. Chitosan is also an antifungal affecting plasma membrane. Fungi with enriched unsaturated free fatty acids in their plasma membrane (increased fluidity) are sensitive to chitosan (e.g. *N. crassa*). In contrast, fungi with less unsaturated free fatty acids in their membranes (low fluidity) such as the nematophagus fungus *Pochonia chlamydosporia,* are resistant to chitosan.[8,27] In our work, we show that chitosan activates genes related with plasma membrane homeostasis such as the class 3 lipase NCU03639 (Fig. 8). The increase on chitosan sensitivity of NCU03639 deletion strain and the induction of genes related with free fatty acid plasma membrane remodeling such as NCU16960 (geranyl reductase), suggests their role in lipid replacement. This group of genes is mainly associated with plasma membrane stabilization by changes in free fatty acid composition caused by other abiotic stresses.[28] Furthermore, chitosan also activated genes related with vesicular transport, which is associated with lipid transfer.[29]

Moreover, chitosan also induced expression of *N. crassa* genes related with movement of molecules through plasma membrane such as MFS transporters. The activation of a monosaccharide transporter and other genes related with exchange of molecules is one of the general responses of *N. crassa* to chitosan. Transport activation

is a widely described response of several filamentous fungi and yeast in response to antifungals.[30] *C. albicans* activates genes involved in transport and molecule trafficking in presence of ketoconazole.[31] Susceptibility to azoles has been likely found due to a reduced efflux activity of pumps.[32] Likewise, amphotericin B induces expression of high-affinity glucose transporters (MFS transporters) and permeases encoding genes in *S. cerevisiae*.[30] In our study, *N. crassa* NCU04537 deletion strain, encoding a monosaccharide transporter, showed an increase in chitosan sensitivity, suggesting a determinant role of this protein in the assimilation of glucosamine and N-acetyl glucosamine monomers.[33]

Currently used antifungals, as well as chitosan, induce intracellular oxidative stress affecting plasma membrane permeability. This may be associated with an imbalance of intracellular redox state.[4,10] An increase in the intracellular ROS is a general response to several antifungals and antimicrobial peptides which target the plasma membrane.[9,34] We have also recently demonstrated that chitosan elicited a rise in ROS coincident with the start of plasma membrane permeabilization.[4] In this paper we have demonstrated that chitosan induced the expression of genes encoding mono- and dioxygenases and other proteins related with ROS homeostasis. Other antifungals (e.g. rotenone and staurosporine) also increase levels of intracellular oxidative stress associated with subsequent cellular death.[35,36] Increase in associated ROS by chitosan could induce plasma membrane free fatty acid oxidation and formation of oxylipins.[37] These would damage plasma membrane and cause its subsequent permeabilization.[38] In our study, when NCU10521, encoding a glutathione S-transferase (GST), was eliminated sensitivity of *N. crassa* to chitosan increased. GST is known to deaden ROS by-products such as peroxidized lipids.[39] This suggests a link between ROS and membrane damage in the mode of action of chitosan (Fig. 8). Other antifungals also induce glutathione enzymes to reduce intracellular ROS levels in *N. crassa*.[40]

We have discovered that chitosan inhibits gene functions related with cytoskeleton dynamics such as microtubule organization and motor activity. Increased levels of intracellular ROS in *Magnaporthe oryzae* caused F-actin depolymerization affecting hyphal polar growth.[41] In *N. crassa* deletion of a NOX gene encoding a NADPH oxidase results in reduction of hyphal growth.[42] These observations support the

hypothesis that an increase in intracellular ROS causes an abnormal distribution of F-actin. Cytoskeleton disorganization could then be one of the mechanisms by which chitosan inhibits fungal growth. The oxidative stress and associated phenomena such as free fatty acid peroxidation or F-actin polymerization could be directly involved in chitosan antifungal activity.

It is known that the balance between Ca^{2+} and ROS affects intracellular signaling and cell homeostasis.[43] We have demonstrated that Ca^{2+} is involved in *N. crassa* tolerance to chitosan. Ca^{2+} is also involved in the increasing threshold of *N. crassa* to antifungals such as staurosporine.[44] Calcium plays a role in the mechanisms of plasma membrane remodeling in *S. cerevisiae* budding[45] and during cell fusion in *N. crassa*.[14,17] In this work, we report NCU10610 (Ca^{2+} regulator with *fig 1* domain) significantly repressed by chitosan. The presence of a *fig 1* domain suggests its role as Ca^{2+} regulator in cell fusion. In view of the relevance of this phenomenon in plasma membrane remodeling, we have also evaluated the role of SYT1 in the mechanisms of plasma membrane remodeling mediated by Ca^{2+}. SYT1 may be involved in membrane damage restored during fusion of germlings in *N. crassa*.[14] In our study Δ*syt1* had increased sensitivity to chitosan. When Δ*syt1* was exposed to chitosan together with Ca^{2+} (10 mM) we found increased sensitivity of this deletion strain to chitosan respect to WT. This would be associated with the capability of this gene to trigger mechanisms of plasma membrane damage repair mediated by Ca^{2+}. Besides, high levels of extracellular Ca^{2+} (20 mM), highly reduced chitosan damage in Δ*syt1*. This deletion strain grow with the same fitness that the WT under these conditions. This would be associated with the activation of other *N. crassa* genes involved in plasma membrane remodeling mediated by Ca^{2+}. Our results would suggest the importance of Ca^{2+} on the mechanisms of plasma membrane remodeling after chitosan damages.

Conclusion and outlook

This work provides the first study of the gene expression response of a filamentous fungus (*N. crassa*) to chitosan. Transcriptomics revealed oxidoreductase activity, membrane homeostasis and microtubule organization as the main gene functions differentially expressed. We identified a class 3 lipase, a MFS monosaccharide

transporter and a glutathione transferase as main gene targets of chitosan in *N. crassa*. Our study opens new possibilities to study gene pathways involved in membrane remodeling after chitosan damage with a relevant role of Ca^{2+}. These studies are a key step to develop chitosan as antifungal drug in the future. Our results could help to identify the main gene targets of chitosan in medical important fungi.

Methods

Growth conditions

Neurospora crassa wild-type strain was 74-OR23-IVA (FGSC2489) and the deletion strains were generated by the *Neurospora* Genome Project[46,47] and kindly provided by the Fungal Genetics Stock Center (FGSC, Kansas, USA)[48] are shown in Table S1. Strains were grown on Vogel's minimal medium agar (VMMA) (1x Vogel's salts, 2% sucrose and 1.5% technical agar).

Chitosan

A medium molecular weight chitosan (70 kDa) with an 82.5% deacetylation degree (T8s; Marine BioProducts GmbH; Bremerhaven, Germany) was used. Chitosan was prepared as described in Palma-Guerrero *et al.*, 2008.[27]

Germinating conditions and time-course of *N. crassa* sensitivity to chitosan

To determine the optimal medium to assess the behavior of *N. crassa* exposed to chitosan, three variants of the Vogel's minimal medium were evaluated (VMM). These media were standard VMM (1x salts, 2% sucrose), VMM salts diluted 100 times with 2% sucrose and VMM salts diluted 100 times and 0.02% sucrose. We finally adopted the second one because chitosan precipitated with some salts included in standard VMM. Time-course experiments of germination were assessed every 2h for 24h under continuous light, shaking at 200 rpm and 25ºC.

N. crassa conidia sensitivity to chitosan was evaluated using selected media, with sub-lethal concentrations of chitosan (0.1-1 μg ml^{-1}). The percentage of *N. crassa* conidial germination with chitosan for 2, 4, 6, 8, 10, 12 and 16h after inoculation was

408 measured. We selected a chitosan dose that resulted in a 50% inhibition of germination
409 respect to the control (IC_{50}).

410 **RNA extraction and cDNA synthesis.**

411 From *N. crassa* cultures in contact with chitosan and controls (without chitosan) for 4,
412 8 and 16h total RNA was isolated using TRIzol reagent (Life Tech) according to the
413 manufacturer's instructions. RNA was then treated with DNase (Turbo DNA-free,
414 Ambion) to eliminate DNA remains. For poly (A+) RNA purification, 10 µg of total
415 RNA was bound to dynal oligo (dT) magnetic beads (Invitrogen) twice, using the
416 manufacturer's instructions. Purified poly (A+) RNA was fragmented by metal-ion
417 catalysis (Ambion) followed by precipitation with 1/10 vol 3M sodium acetate and 3×
418 vol 100% ethanol. Precipitated RNA was 70% ethanol washed and then resuspended
419 into 10.5 µl nuclease free water. For first strand cDNA synthesis, the fragmented poly
420 (A+) RNA was incubated with 3 µg random hexamers (Invitrogen), incubated at 65°C
421 for 5 min and then transferred to ice. First strand buffer (4 µL; Invitrogen),
422 Dithiothreitol (DTT), dNTPs and RNAseOUT (Invitrogen) were added to a final
423 concentration of 1×, 10 mM, 200 µM and 1U/µL, respectively in a final volume of 20 µl
424 and the samples were incubated at 25°C for 2 minutes. Superscript II (200 U;
425 Invitrogen) were added and the samples were incubated at 25°C for 10 min, 42°C for 50
426 min and 70°C for 15 min. For second strand synthesis, 51 µL of H_2O, 20 µL of 5×
427 second strand buffer (Invitrogen), and dNTPs (10 mM) were added to the first cDNA
428 strand synthesis mix and incubated on ice for 5 min. RNaseH (2 U; Invitrogen), DNA
429 pol I (50 U; Invitrogen) were then added and the mixture was incubated at 16°C for
430 2.5h.

431 **Library construction and sequencing**

432 End-repair was performed by adding 45 µL of H_2O, T4 DNA ligase buffer with 10 mM
433 ATP (NEB; 10 µL), dNTP mix (10 mM), T4 DNA polymerase (15 U; NEB), Klenow
434 DNA polymerase (5 U; NEB), and T4 PNK (50 U; NEB) to the sample and incubating
435 for 30 min at 20°C. A single base was added each to cDNA fragment by adding Klenow
436 buffer (NEB), dATP (1 mM), and Klenow 3′ to 5′ exo- (15 U; NEB). The mixture was
437 then incubated at 37°C for 30 min. Standard Illumina adapters (FC) were ligated to the

cDNA fragments using 2× DNA ligase buffer (Enzymatics), 1 µL of adapter oligo mix and DNA ligase (5 U; Enzymatics). The sample was incubated at 25°C for 15 min. The sample was purified in a 2% low-melting point agarose gel, and a slice of gel containing 200-bp fragments was removed and the DNA purified. The polymerase chain reaction (PCR) was used to enrich the sequencing library. A 10 µL aliquot of purified cDNA library was amplified by PCR using the pfx DNA polymerase (2 U; Invitrogen) and with 1 µl of genomic primers 1.1 and 2.1 (Illumina). PCR cycling conditions included a denaturing step at 98°C for 30 sec, 12 cycles of 98°C for 10 sec, 65°C for 30 sec, 68°C for 30 sec, and a final extension at 68°C for 5 min. All libraries were sequenced on a HiSeq 2000 platform to a depth of over 190 million 50 bp reads using standard Illumina operating procedures.

Transcript abundance, annotation and functional analysis.

Sequenced libraries were mapped against predicted transcripts from the *Neurospora crassa* OR74A genome (v10) with TopHat (v2.0.4)[49] and the short sequence aligner Bowtie (v2.0.0.6).[50] Transcript abundance measured as FPKMs (Fragments Per Kilobase transcript model per Million fragments mapped) was calculated with Cufflinks (v 2.0.2) using counts that exclusively mapped to predicted transcripts to estimate the FPKM denominator. Genes which had a differential expression cut-off of p-value < 0.05 (we adjusted p-value as the Benjamini Hochberg filter; q value in TopHat; to adjust for the false discovery rate) between control and sample were used for further analysis. In the fold change analysis a lo_2foldchange ≥ 2 was adopted to characterize the main gene functions and genes involved in the response of *N. crassa* to chitosan. The project of *N. crassa* gene expression profile in response to chitosan has been deposited in NCBI's Gene Expression Omnibus[51] and is accessible through GEO Series accession number GSE75293 (https://www.ncbi.nlm.nih.gov/geo/query/acc.cgi?acc=GSE75293).

N. crassa transcript sequences were re-annotated using Blast2GO software (Version 2.7.1) to improve the standard annotation provided by the Broad *N. crassa* genome (http://www.broadinstitute.org/annotation/genome/neurospora/MultiHome.html), a consensus set of transcripts were functionally annotated (gene ontology, GO) using Blast2GO (http://www.blast2go.com/b2ghome).[52] Gene families were established using

the InterPro (http://www.ebi.ac.uk/interpro) and KEGG databases (http://www.genome.jp/kegg/pathway.html). For *N. crassa* gene annotation we also used several tools, HMMR[53] including Pfam, TIGRFAM, Gene 3D and Superfamily databases. In addition, Wolf PSORT[54] was used to obtain information about domains and cellular gene localizations. Gene annotations were finally examined using BLASTp.[55]

RNA-seq time-series data analysis

Significant differential gene expression changes over time were assessed by applying the maSigPro R package[21] to the groups of genes included in each functional GO category. This approach was described, as an adaptation of maSigPro[56] named maSigFun[24] for microarray data. This algorithm has been updated for RNA-seq data in this work. The maSigPro method follows a two-stage regression strategy to identify genes with significant changes in expression over time. False discovery rate (FDR) and R^2 level as measure of the good of fit of the regression model are the factors for gene selection. Finally the package includes several clustering algorithms and visualization tools available to group and display the selected gene-profiles.

Transcriptional responses of interest were detected with the application of ASCA-genes method.[22] Considering an experiment with 2 factors (a and b, usually time and the experimental group, in our case chitosan treatment), data can be collected in a data matrix X, where rows represent samples and columns represent genes. ASCA first decomposes X into matrices (X_a, X_b and X_{ab}) with the estimates of the ANOVA (Analysis of Variance) parameters: X_a contains the time effects, X_b treatment effects and X_{ab} the interactions, obtained gene by gene. When the main interest of a study is the identification of genes with differences in the experimental groups, X_b is joined to X_{ab}. Principal Component Analysis (PCA) is then applied on each of these matrices to summarize the information of each source of variation and giving as a result two PCA analyses that are called submodels. ASCA-genes compute the main patterns of variation and two statistics for each gene in each submodel: leverage and the squared-prediction error (SPE). Leverage indicates the importance of a gene in the main behavior discovered. SPE quantifies the variability of a gene that is not detected for the model.

Focusing on these measures, ASCA-genes provides two lists of genes: the first one with genes that follow the main general patterns. The second one including genes with odd behaviors or outlier data. To obtain this gene selection the gamma method[57] was applied.

Real time quantitative PCR for RNA-seq validation

cDNA was synthetized with a retro-transcriptase RevertAid (Thermo) using oligo dT (Thermo). Gene expression was quantify using real-time reverse transcription PCR (qRT-PCR), SYBR Green with ROX (Roche) were used following the manufacturer's instructions. Gene quantifications were performed in a Step One Plus real-time PCR system (Applied Biosystems). Relative gene expression was estimated with the ΔΔCt methodology,[58] with three technical replicates per condition. Primers used to quantify the expression of genes related with *N. crassa* response to chitosan are shown in Table S4. Expression of the TATA-binding protein (NCU04770) and transcription elongation factor S-II (NCU02563) were used as endogenous controls for all experiments, since these genes showed Ct stability for all conditions tested.

Evaluation of selected deletion strains to determine the genes involved in the response of *N. crassa* to chitosan

Experiments in liquid media were set to evaluate growth kinetics of *N. crassa* (WT) and selected homokaryons deletion strains (Table S1). *N. crassa* conidia were obtained from 8-10 day-old sporulated cultures, by adding 2 ml of distilled water. The resulting conidial suspensions were then filtered through Miracloth (Calbiochem) to remove hyphal fragments. Conidial suspensions were adjusted to a final concentration of 10^6 conidia ml^{-1} with 1/100 VMM salts and 2% sucrose.

Chitosan (1-6 μg ml^{-1}) was added to the medium and 200 μL per well were dispensed into 96 well microtiter plates (Sterillin Ltd., Newport, UK). Plates were inoculated with *N. crassa* conidia (2×10^5 conidia per well) and then incubated at 25 ºC during 48h in a GENios^{TM} multiwell spectrophotometer (Tecan, Männedorf, Switzerland) in the dark. The chitosan effect on growth of *N. crassa* strains was evaluated by measuring optical density at 490 nm (OD_{490}).[4] In order to identify the antifungal activity of chitosan on *N.*

crassa strains, we applied a spot assay in SFG medium (2% sorbose, 0.05% glucose and fructose and 1.5% agar).[59]

Growth in presence of the same concentration of deletion strains (mating type a) to chitosan was confirmed by segregation analysis.[60] Ascospore progeny were selected from crosses with FGSC 2489 (mating type A). Seggregants were tested both for chitosan and hygromycin sensitivity. The latter was tested in all deletion strains used in this work. Seggregants had the same chitosan sensitivity than the original deletion strain and were hygromycin (200 μg ml^{-1}) resistant.

Evaluation of the effect of Ca^{2+} in the response of *N. crassa* to chitosan

To evaluate the effect of Ca^{2+} on conidia treated with chitosan, we exposed *N. crassa* conidia (10^6 conidia ml^{-1}) to chitosan (0.5 μg ml^{-1}) with either 0.17; 0.34; 0.68; 1.36 or 2.72 mM $CaCl_2$. Growth kinetics was evaluated in a 96-multiwell microplate by measuring optical density at 490 nm for 48h, as described above.

Viability of conidia was determined using propidium iodide (PI; Sigma)[7] after exposure to chitosan (0.5 μg ml^{-1}), and $CaCl_2$ at 0.68 mM, conidia without $CaCl_2$ were used as a controls for this compound. *N. crassa* conidia were treated with chitosan for 2 h and then labeled with 2 μg ml^{-1} PI to evaluate cell viability. Fluorescence in conidia was assessed using an Olympus BH-2 fluorescence microscope with 488 nm and 560 nm as excitation and detection wavelengths, respectively, and then photographed with a Leica DFC480 digital camera (Leica Microsystems, Wetzlar, Germany).

The effect of higher concentrations of Ca^{2+} (10 and 20 mM) on WT and two deletion strains, ΔNCU10610 (Ca^{2+} regulator with *fig 1* domain) and ΔNCU03263 (*syt1*) when combined with chitosan (4 μg ml^{-1}) was also determined.

Cytoscape network of functional gene annotation of *N. crassa* gene response to chitosan

For this analysis, we performed functional enrichment analysis with GSEA (Gene Set Enrichment Analysis).[61] The enrichment maps were generated with Enrichment Map Plugin v1.1[62] developed for Cytoscape.[23] Nodes in the maps were clustered with the

Markov clustering algorithm, using an overlap coefficient computed by the plugin as the similarity metric (coefficient < 0.5 were set to zero) and an inflation parameter with value of 2. For each cluster, the leading edge was computed as in Subramanian *et al.* (2005)[61] for each member of a node. A complete functional gene network map of *N. crassa* in response to chitosan was finally generated.

Acknowledgements

This work was supported by the National Institutes of Health (USA) grant GM060468 to NLG and Spanish Ministry of Economy and Competitiveness Grant AGL 2011-29297/AGR to LVLL.

We thank help from Dr. Maria DLA Jaime (University of National Institutes of Health–NIDDK, Bethesda, USA) with GSEA and Cytoscape analyses. We also thank support from BioBam Bioinformatics (Valencia, Spain) to use Blast2GO Pro. We also wish to thank Ms. Nuria Escudero (University of Alicante) for her critical comments of the manuscript.

References

1. R.M.N.V. Kumar, *React. Funct. Polym.*, 2000, **46** (1): 1-27.
2. C.R. Allan, and L.A. Hadwiger, *Exp. Mycol.*, 1979, **3** (3): 285-287.
3. S.N. Kulikov, S.A. Lisovskaya, P.V. Zelenikhin, E.A. Bezrodnykh, D.R. Shakirova, I.V. Blagodatskikh, V.E. Tikhonov, *Eur. J. Med. Chem.*, 2014, **74:** 169-178.
4. F. Lopez-Moya, M.F. Colom-Valiente, P. Martinez-Peinado, J.E. Martinez-Lopez, E. Puelles, J.M. Sempere-Ortells, L.V. Lopez-Llorca, *Fun. Biol.*, 2015, **119** (2-3): 154-169.
5. M.D.L.A. Jaime, L.V. Lopez-Llorca, A. Conesa, A.Y. Lee, M. Proctor, L.E. Heisler, M. Gebbia, G. Giaever, J.T. Westwood, C. Nislow, *BMC Genomics*, 2012, **13** (1): 267.

6. A. Zakrzewska, A. Boorsma, S. Brul, K.J. Hellingwerf, F.M. Klis, *Eukaryot. Cell.*, 2005, **4** (4): 703–715.

7. J. Palma-Guerrero, I.C. Huang, H-B. Jansson, J. Salinas, L.V. Lopez-Llorca, and N.D. Read, *Fungal Genet. Biol.*, 2009, **46** (8): 585–594.

8. J. Palma-Guerrero, J.A. Lopez-Jimenez, A.J. Pérez-Berná, I. Huang, H-B. Jansson, J. Salinas, J. Villalaín, N.D. Read, L.V. Lopez-Llorca, *Mol. Microbiol.*, 2010, **75** (4): 1021-1032.

9. M.A. Ghannoum and L.B. Rice, *Clin. Microbiol. Rev.*, 1999, **12** (4): 501-517.

10. I.E.J.A. François, B.P.A. Cammue, M. Borgers, J. Ausma, G.D. Dispersyn, K. Thevissen, *Antiinfect. Agents Med. Chem.*, 2006, **5** (1): 3-13.

11. N. Delattin, B.P. Cammue, K. Thevissen, *Future Med. Chem.*, 2014, **6** (1): 77-90.

12. N.W. Andrews, P.E. Almeida, M. Corrotte, *Trends Cell Biol.*, 2014, **24** (12): 734-742.

13. K.D. Brewer, T. Bacaj, A. Cavalli, C. Camilloni, J.D. Swarbrick, J. Liu, A. Zhou, P. Zhou, N. Barlow, J. Xu, A.B. Seven, E.A. Prinslow, R. Voleti, D. Häussinger, A.M. Bonvin, D.R. Tomchick, M. Vendruscolo, B. Graham, T.C. Südhof, J. Rizo, *Nat. Struct. Mol. Biol.*, 2015, **22** (7): 555-564.

14. J. Palma-Guerrero, A.C. Leeder, J. Welch, N.L. Glass, *Mol. Microbiol.*, 2014, **92** (1): 164-182.

15. A.P. Gonçalves, J.M. Cordeiro, J. Monteiro, C. Lucchi, P. Correia-de-Sá, A. Videira, *Biochim. Biophys. Acta.*, 2015, **1847** (10): 1064-1074.

16. E.M. Muller, N.A. Mackin, S.E. Erdman, K.W. Cunningham, *J. Biol. Chem.*, 2003, **278** (40): 38461-38469.

17. A. Fleissner, S. Diamond, N.L. Glass, *Genetics*, 2009, **181** (2): 497–510.

18. B. Cavinder F. Trail, *Eukaryot. Cell.*, 2012, **11** (8): 978-988.

19. M.Á. Curto, M.R. Sharifmoghadam, E. Calpena, N. De León, M. Hoya, C. Doncel, J. Leatherwood, M.H. Valdivieso, *Genetics*, 2014, **196** (4):1059-1076

20. J. Palma-Guerrero, J. Zhao, A.P. Gonçalves, T.L. Starr, N.L. Glass, *Eukaryot. Cell*., 2015, **14** (3): 265-277.

21. M.J. Nueda, S. Tarazona, A. Conesa, *Bioinformatics*, 2014, **30** (18): 2598-2602.

22. M.J. Nueda, A. Conesa, J.A. Westerhuis, H.C.J. Hoefsloot, A.K. Smilde, M. Talón, A. Ferrer, *Bioinformatics*, 2007, **23** (14): 1792-1800.

23. M.E. Smoot, K. Ono, J. Ruscheinski, P.L. Wang, T. Ideker, *Bioinformatics*, 2011, **27** (3): 431–432.

24. M.J. Nueda, P. Sebastián, S. Tarazona, F. García-García, J. Dopazo, A. Ferrer, A. Conesa, *BMC-Bioinfo*., 2009, **10** (6): S9.

25. F.C. Odds, A.J. Brown, N.A. Gow, *Trends Microbiol*., 2003 **11** (6): 272-279.

26. A.J. Carrillo-Muñoz, G. Giusiano, P.A. Ezkurra, G. Quindós, *Rev. Esp. Quimioter*., 2006, **19** (2): 130-139.

27. J. Palma-Guerrero, H-B. Jansson, J. Salinas, L.V. Lopez-Llorca, *J. Appl. Microbiol*., 2008, **104** (2): 541-553.

28. L.N. Nguyen, A. Gacser, J.D. Nosanchuk, *Virulence*, 2011, **2** (6): 538-541

29. Schauder, C.M., Wu, X., Saheki, Y., Narayanaswamy, P., Torta, F., Wenk, M.R., De Camilli, P., and Reinisch, K.M. *Nature,* 2014, **510** (7506): 552-555.

30. A.K. Agarwal, P.D. Rogers, S.R. Baerson, M.R. Jacob, K.S. Barker, J.D. Cleary, L.A. Walker, D.G. Nagle, A.M. Clark, *J. Biol. Chem*., 2003, **278** (37): 34998-5015.

31. C.F. Hoehamer, E.D. Cummings, G.M. Hilliard, P.D. Rogers, *Antimicrob. Agents. Chemother*., 2010, **54** (5): 1655-1664.

32. E. Thomas, E. Roman, S. Claypool, N. Manzoor, J. Pla, S.L. Panwar, *Antimicrob. Agents. Chemother*., 2013, **57** (11):5580-99

630 33. H.L. Mobley, R.J. Doyle, U.N. Streips, S.O. Langemeier, *J. Bacteriol*., 1982, **150**
631 (1): 8-15.

632 34. B.M. Hayes, M.A. Anderson, A. Traven, N.L. van der Weerden, M.R. Bleackley,
633 *Cell. Mol. Life Sci.*, 2014, **71** (14): 2651-2666.

634 35. A. Castro, C. Lemos, A. Falcão, A.S. Fernandes, N.L. Glass, A. Videira, *Eukaryot.*
635 *Cell*., 2010, **9** (6): 906-914.

636 36. A.P. Gonçalves, C. Hall, D.J. Kowbel, N.L. Glass, A. Videira, *G3 (Bethesda)*,
637 2014, **4** (6): 1091-102.

638 37. F. Brodhun, I. Feussner, *FEBS J.*, 2011, **278** (7): 1047-1063.

639 38. A. Singh, M. Del Poeta, *Cell Microbiol*., 2011, **13** (2): 177-85.

640 39. Y. Yang, J.Z. Cheng, S.S. Singhal, M. Saini, U. Pandya, S. Awasthi, Y.C. Awasthi,
641 *J. Biol. Chem*., 2010, **276** (22): 19220-19230.

642 40. A.S. Fernandes, A. Castro, A. Videira, *Apoptosis*, 2013, **18** (8): 940-8.

643 41. L.S. Ryder, Y.F. Dagdas, T.A. Mentlak, M.J. Kershaw, C.R. Thornton, M. Schuster,
644 J. Chen, Z. Wang, N.J. Talbot, *Proc. Natl. Acad. Sci. USA*., 2013, **110** (8): 3179-
645 3184.

646 42. N. Cano-Domínguez, K. Álvarez-Delfín, W. Hansberg, J. Aguirre, *Eukaryot. Cell*.,
647 2008, **7** (8): 1352-1361.

648 43. Y. Yan, C.L. Wei, W.R. Zhang, H.P. Cheng, J. Liu, (2006) *Acta Pharmacol. Sin*.,
649 2006, **27** (7): 821-826.

650 44. A.P. Gonçalves, , J. Monteiro, , C. Lucchi, , D.J. Kowbel, , J.M. Cordeiro, , P.
651 Correia-de-Sá, , D.J. Rigden, N.L. Glass, A. Videira, *Microbial Cell.*, 2014, **1** (9):
652 289-302

653 45. P. D'hooge, C. Coun, V. Van Eyck, L. Faes, R. Ghillebert, L. Mariën, J.
654 Winderickx, G. Callewaert, *Cell Calcium*, 2015, **58** (2): 226-235.

655 46. H.V. Colot, G. Park, G.E. Turner, C. Ringelberg, C.M. Crew, L. Litvinkova, RL
656 Weiss, K.A. Borkovich, J.C. Dunlap. *Proc. Natl. Acad. Sci. USA*., 2006, **103** (27):
657 10352-10357.

658 47. J.C. Dunlap, K.A. Borkovich, M.R. Henn, G.E. Turner, M.S. Sachs, N.L. Glass, K.
659 McCluskey, M. Plamann, J.E. Galagan, B.W. Birren, R.L. Weiss, J.P.
660 Townsend, J.J. Loros, M.A. Nelson, R. Lambreghts, H.V. Colot, G. Park, P.
661 Collopy, C. Ringelberg, C. Crew, L. Litvinkova, D. DeCaprio, H.M. Hood, S.
662 Curilla, M. Shi, M. Crawford, M. Koerhsen, P. Montgomery, L. Larson, M.
663 Pearson, T. Kasuga, C. Tian, M. Baştürkmen, L. Altamirano, J. Xu, *Adv. Genet*.,
664 2007, **57**:49-96.

665 48. K. McCluskey, *Adv. Appl. Microbiol*., 2003, **52**: 245-262.

666 49. C. Trapnell, L. Pachter, S.L. Salzberg, *Bioinformatics,* 2009, **25** (9):1105-1111.

667 50. B. Langmead, C. Trapnell, M. Pop, S.L. Salzberg, *Genome Biol.,* 2009, **10** (3):R25

668 51. A. Conesa, S. Götz, *Int. J. Plant Genomics*, 2008, 2008:619832.

669 52. R. Edgar, M. Domrachev, A.E. Lash, *Nucl. Ac. Res,* 2002, **30** (1):207-210.

670 53. R.D. Finn, J. Clements, S.R. Eddy, *Nucl. Ac. Res.*, 2011, **39**: 29-37.

671 54. P. Horton, K.J. Park, T. Obayashi, N. Fujita, H. Harada, C.J. Adams-Collier, K.
672 Nakai, *Nucleic. Acids. Res*., 2007, W585-587.

673 55. W. Gish, D.J. States, *Nature Genet*., 1993, (3): 266-272.

674 56. A. Conesa, M.J. Nueda, A. Ferrer, M. Talon, *Bioinformatics*, 2006, **22** (9): 1096-
675 1102**.**

676 57. S. Tarazona, S. Prado-López, J. Dopazo, A. Ferrer, A. Conesa, *Chemometr. Intell.*
677 *Lab. Syst*., 2012, **100**: 113-122.

678 58. K.J. Livak, T.D. Schmittgen, *Methods*, 2001, 25: 402-408.

679 59. H.E. Brockman, F.J. de Serres, *Genetics*, 1963, **48** (4): 597-604.

60. A.C. Leeder, W. Jonkers, J. Li, N.L. Glass, *Genetics*, 2013, **195** (3): 883-898.

61. A. Subramanian, P. Tamayo, V.K. Mootha, S. Mukherjee, B.L. Ebert, M.A. Gillette, A. Paulovich, S.L. Pomeroy, T.R. Golub, E.S. Lander, J.P. Mesirov, *Proc. Natl. Acad. Sci. USA*, 2005, **102** (43): 15545–15550.

62. D. Merico, R. Isserlin, O. Stueker, A. Emili, G.D. Bader, *PLoS One*, 2010, **5** (11): e13984.

Figure legends

Figure 1. Time-course effect of chitosan on *N. crassa* conidia germination. **(A)** *N. crassa* germination started prior to 4h then conidia develop a germ tube (6-8h) and established a young mycelium before 16h. **(B)** Effect of chitosan on conidia germination at 8h, IC_{50} (50% germination) was found at 0.5 µg ml^{-1} chitosan. IC_{50}: half maximal inhibitory concentration.

Figure 2. Venn diagram of differential gene expression of *N. crassa* in response to chitosan. **(A)** Complete differential gene expression (DGE) including induced and repressed genes in the 4-16h time-course. **(B)** Increased DGE, up-regulated genes. **(C)** Decreased DGE, down-regulated genes. **(D)** Fold-change of 22 genes significantly differentially expressed in response to chitosan during the whole time-course expermient.

Figure 3. Gene Ontology (GO) functional annotation of *N. crassa* genes differentially expressed in response to chitosan. **(A)** Global GO annotation of significantly expressed genes. **(B)** Selected GO-terms time-series with maSigFun represented as the average expression profile of the associated genes to each GO.

Figure 4. (A-D) Time-series analysis of genes associated with the response of *N. crassa* to chitosan by ASCA-genes. Graphs represent gene expression average trend of four clusters of genes that follow the discovered general patterns of the ASCA model. Genes that are well represented by the PC obtained with the ASCA model.

Figure 5. Effect of chitosan on growth of *N. crassa* WT and selected deletion strains from RNAseq data. **(A)** Chitosan minimal inhibitory concentration (MIC) of selected deletion strains and WT. **(B-E)** Fungal growth kinetics of **(B)** WT, **(C)** ΔNCU03639, **(D)** ΔNCU04537 and **(E)** ΔNCU08770 in response to increasing concentrations of chitosan (n=4; mean ± SE).

Figure 6. Effect of Ca^{2+} on chitosan antifungal activity to *N. crassa* WT and deletion strains from membrane remodeling genes (ΔNCU10610 and ΔNCU03263-Δ *syt 1*). (A) *N. crassa* WT growth in response to chitosan (0.5 µg ml-1) under several Ca^{2+} concentrations. (B) Nuclear damage after treatment of conidia of a strain in which PI has been targeted to the nuclei. Conidia treated with chitosan and stained with 2 µg ml^{-1} propidium iodide (PI). Fluorescence images right and DIC images of same conidia on the left. Bar = 5 µm. (C) Evaluation of conidia viability treated with chitosan and Ca^{2+} stained with PI.

Figure 7. Cytoscape network of functional gene annotation of *N. crassa* gene response to chitosan. Large font tittles represents a summary of GO-terms found enriched in clusters. Node size correlates to the number of genes annotated to that functional category. Each node represents a gene function significantly enriched (FDR≤ 0.1).

Figure 8. Key genes associated with *N. crassa* response to chitosan. In this model, NCU03639 would increase membrane permeability by altering mechanisms of plasma membrane remodeling and fluidity. NCU10610 (Ca^{2+} regulator with *fig 1* domain) would be associated with the mechanisms of plasma membrane remodeling mediated by Ca^{2+}. NCU04534 (MFS transporter) could be involved in mechanisms of assimilation or detoxification monosaccharaides (e.g. monomers of N-acetyl glucosamine). NCU10521 (glutathione transferase), NCU01849 and NCU01071 (dioxygenases) would be related with the response of the fungus to the oxidative stress, the key response of *N. crassa* to chitosan. Genes involved in mechanisms associated with protein synthesis (NCU04555) and resistance to chemical compounds (NCU02363) are also differentially expressed in response to chitosan.

737

738

739

740

741

742

Fig. 1

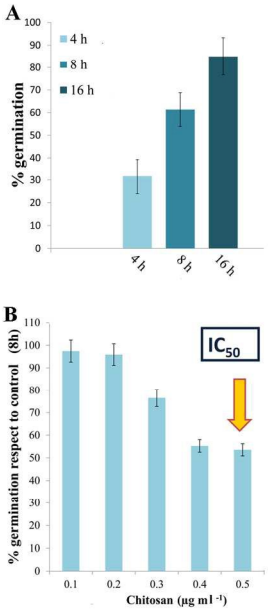

209x270mm (254 x 254 DPI)

Fig. 2

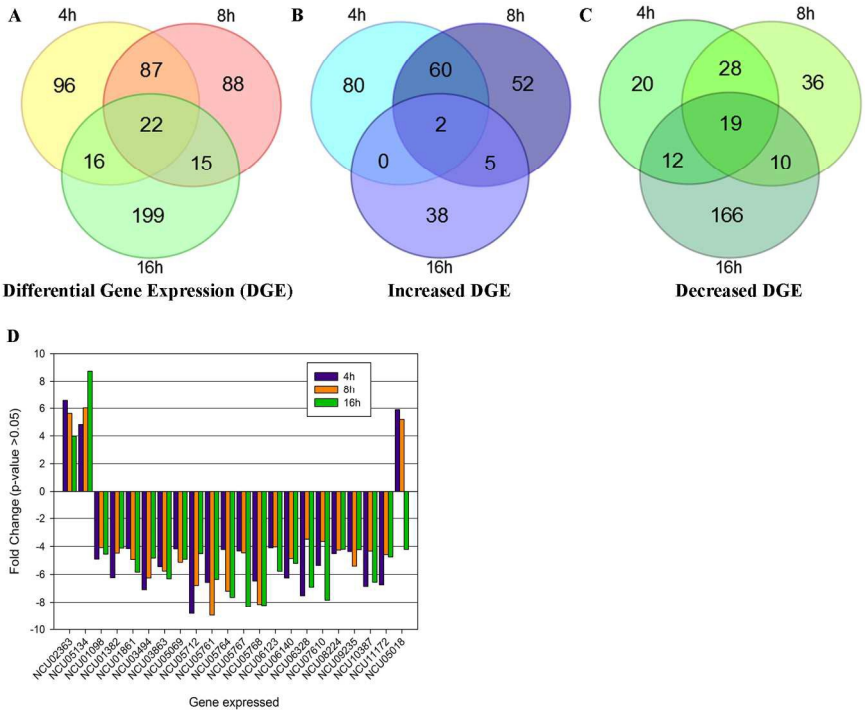

209x270mm (254 x 254 DPI)

Fig. 3

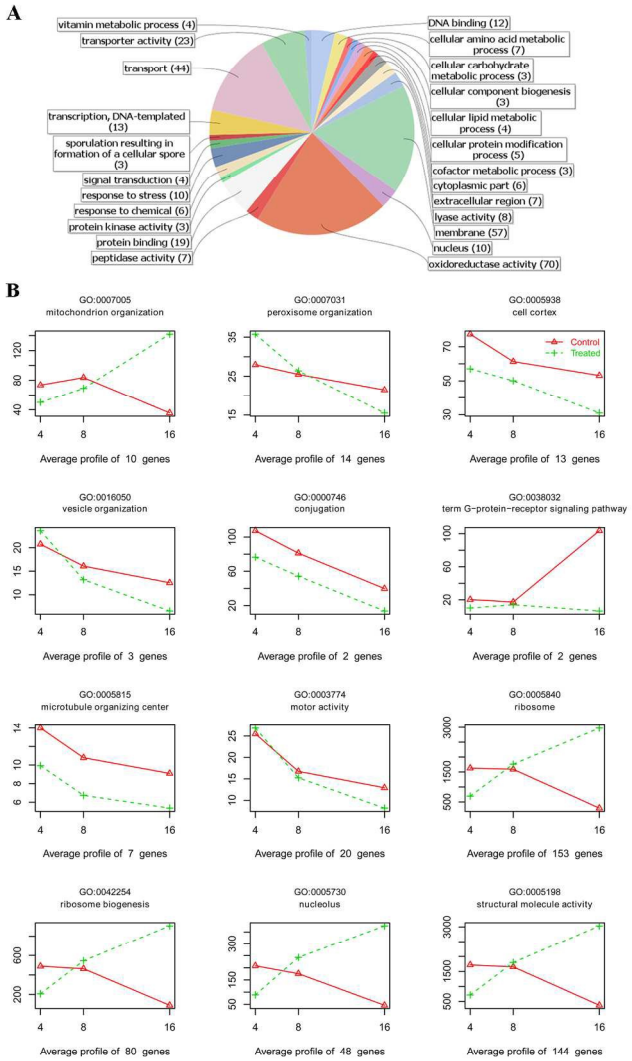

209x270mm (254 x 254 DPI)

Fig. 4

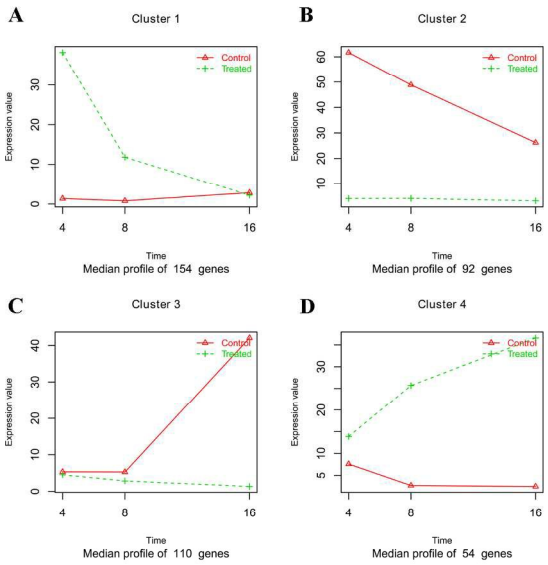

209x270mm (254 x 254 DPI)

Fig. 5

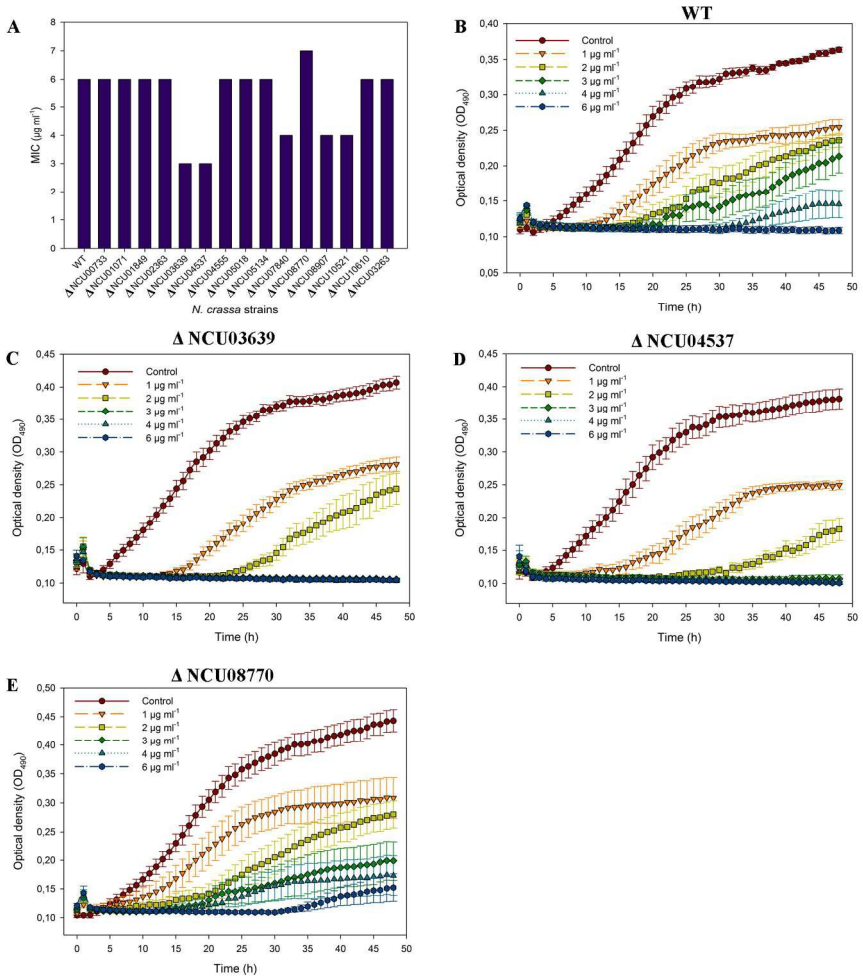

209x270mm (254 x 254 DPI)

Fig. 6

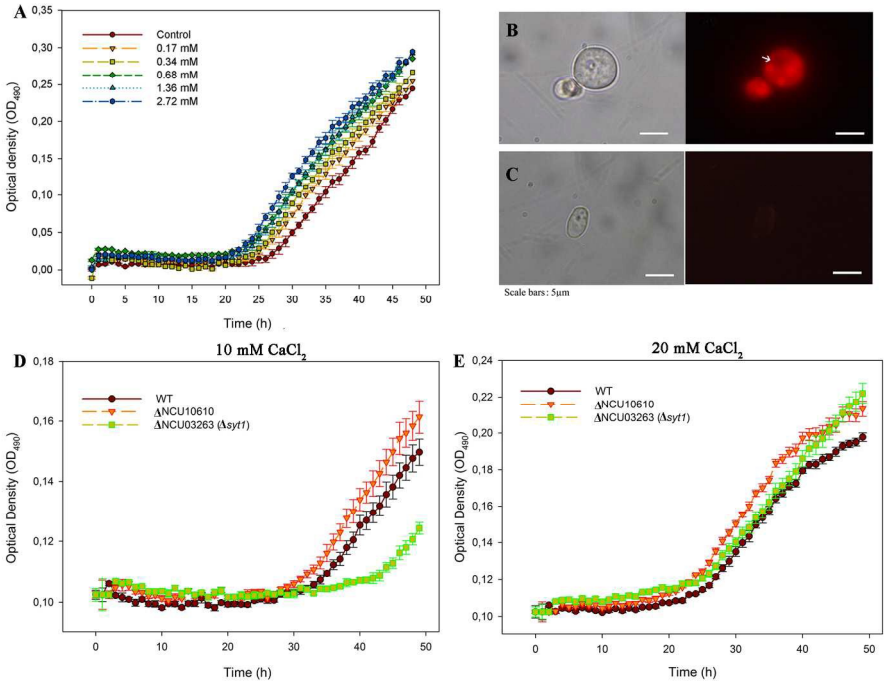

209x270mm (254 x 254 DPI)

Fig. 7

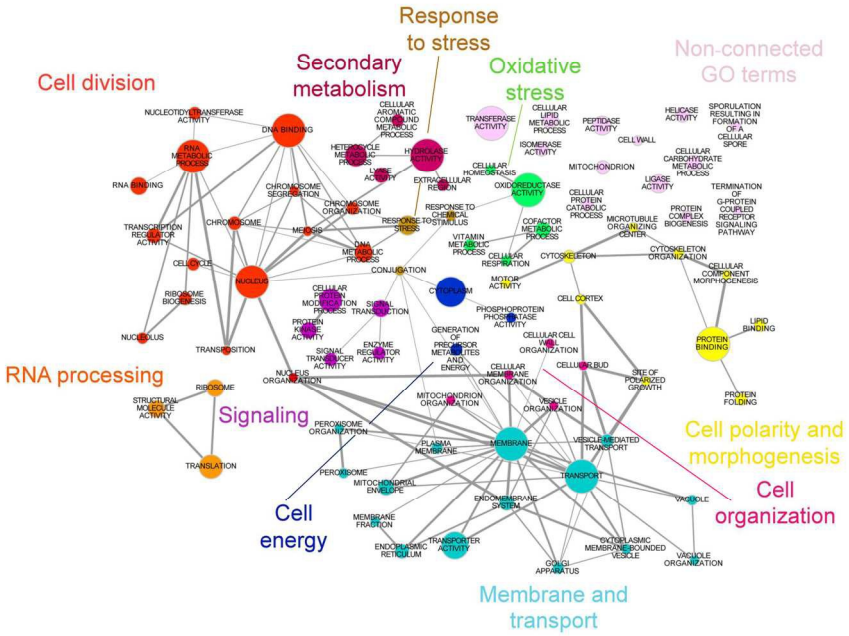

209x270mm (254 x 254 DPI)

Fig. 8

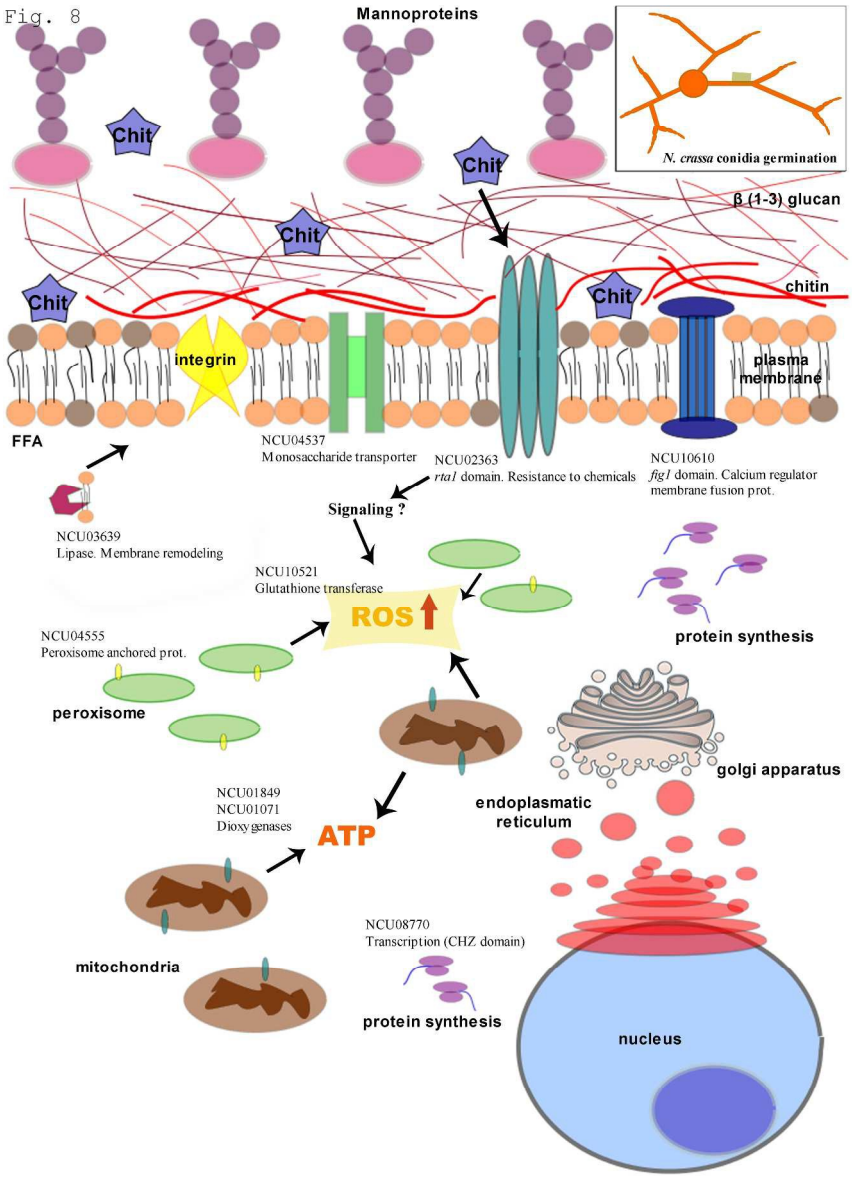

371x525mm (300 x 300 DPI)